

# Enhanced Velocity Sensitivity in 4-D FMCW LiDAR by Use of Avalanche Photodiode with Cascaded Multiplication Layer

Zohauddin Ahmad<sup>1</sup>, Sung-Yi Ou<sup>1,2</sup>, Wei-Chih Su<sup>3</sup>, Po-Shun Wang<sup>1</sup>, Naseem<sup>1</sup>, Jyehong Chen<sup>4</sup>, Yung-Jr Hung<sup>2</sup>, You-Chia Chang<sup>4\*\*\*\*</sup>, Chia-Chien Wei<sup>2\*\*</sup>, Tzyy-Sheng Horng<sup>3\*\*\*</sup>, and Jin-Wei Shi<sup>1\*</sup>

<sup>1</sup>Department of Electrical Engineering, National Central University, Taoyuan 320, Taiwan

\*Tel: +886-3-4227151 ext. 34466, \*FAX: +886-3-4255830

\*Email: [jwshi@ee.ncu.edu.tw](mailto:jwshi@ee.ncu.edu.tw)

<sup>2</sup>Department of Photonics, National Sun Yat-sen University, Kaohsiung, Taiwan.

\*\*Email: [ccwei@mail.nsysu.edu.tw](mailto:ccwei@mail.nsysu.edu.tw)

<sup>3</sup>Department of Electrical Engineering, National Sun Yat-Sen University, Kaohsiung, Taiwan

\*\*\*Email: [jason@ee.nsysu.edu.tw](mailto:jason@ee.nsysu.edu.tw)

<sup>4</sup>Department of Photonics, National Yang Ming Chiao Tung University, Hsinchu, Taiwan

\*\*\*\*Email: [youchia@nycu.edu.tw](mailto:youchia@nycu.edu.tw)

**Abstract:** A 4-D FMCW LiDAR is demonstrated. In comparison to the traditional p-i-n PD in its receiver-side, the cascaded M-layers APDs provide a better quality of 4-D images with unprecedented high velocity-sensitivity (5 $\mu$ m/sec) for slow-moving objects.

©2023 Optical Society of America

**OCIS codes:** (230.5170) Photodiodes (230.0040) Detectors

## I. Introduction

Ever since outbreak of the pandemic, there has been tremendous research on the contactless healthcare with a focus on the development of contactless sensor technologies that eliminate the need for physical interactions between patients and healthcare professionals. Among the reported solutions, frequency modulated continuous wave (FMCW) radar technology attracts most of the attentions and has been commercialized to remotely monitor and measure the object's slow-moving speed and vital signs (VSM) [1]. However, obtaining a real-time 4D (3D + velocity) image based on the FMCW radar scheme with a compact antenna size remains a challenge. FMCW LiDAR, which merges the FMCW radar architecture with the additional electrical-to-optical (EO) and optical-to-electrical (OE) conversion modules, has been demonstrated to be one of the most effective solutions to accomplish such goal [2]. However, these additional energy conversion processes in LiDAR leads to a larger phase noise and the broadening of baseband signal at its receiver-end. This severely limits its capability to resolve the minor Doppler frequency shift for high velocity sensitivity and VSM application. In this work, we combine the self-injection-locked (SILO) radio-frequency (RF) Oscillator [3] with our home-made avalanche photodiode (APD) [4], which has unique design of cascaded multiplication (M-) layer and excellent performance in terms of saturation current and responsivity, in the 4-D FMCW LiDAR system to minimize the phase and amplitude noises at the receiver-end. In contrast to the traditional p-i-n PD receiver, our home-made APD can produce a higher quality 4-D (3-D + instantaneous velocity) images with record-high velocity sensitivity (5  $\mu$ m/sec) for slow-moving objects among all the reported 4-D FMCW LiDARs [5-8].

## II. System Setups

Figure 1 shows the setup of our FMCW LiDAR system. The receiver-end in our LiDAR must be able to discern the minor Doppler frequency shift ( $f_D$ ) down to the few Hz level in order to achieve the ultimate high velocity sensitivity. Here, the heterodyne scheme is adopted to overcome the problem of laser flicker noise in the low-frequency regime. Thus, the frequency of the FMCW laser (Alnair Labs ASE-200) is additionally up-converted by 2.4 GHz (i.e., the intermediate frequency, denoted by IF) using a single-sideband (SSB) Mach-Zehnder modulator (MZM), which is driven by a RF local oscillator (LO) at 2.4 GHz. For comparison, two kinds of photodetectors in the receiver-end are adopted. One is our home-made avalanche photodiode (APD) with cascaded multiplication layers [4]. This design leads to superior performance in terms of the responsivity and saturation current to those of p-i-n PDs for the FMCW LiDAR applications [4]. The other one is a commercially available p-i-n PDs based Rx (Picometrix PT-40D/8XLMD), which is composed of a high-speed p-i-n PD integrated with a trans-impedance amplifier (TIA). After the APD or PD, the signal is down-converted to the baseband using the LO and a quadrature mixer, as shown in Fig. 1. Moreover, since the SILO RF oscillator can provide the additional gain in the signal-to-noise (S/N) ratio in FMCW radar system [3], particularly for a weak low-frequency signal detection, we adopt such scheme in our receiver-end to improve the quality of obtained 4-D images. As shown in Fig. 1, to realize RF self-injection in the receiver-end, the beating signal between the echo light and reference light is injected into the LO to modulate its output frequency, resulting in the LO operating as a SILO. A frequency demodulator composed of a mixer and a delay line is then used to extract the Doppler frequency shift from the LO output signal. To illuminate the object, we use a fiber collimator based FMCW LiDAR system. The mechanical sweeping mirror inside allows beam scanning with a field-of-view of  $\pm 12.5^\circ$  and a repeatability of 15  $\mu$ rad. The light reflected by the object is received by the same fiber collimator, and a circulator is used to redirect the reflected light toward the APD for feeding the SILO loop. The down-converted in-phase and quadrature data ( $I$  and  $Q$ ), which are recorded by a real-time oscilloscope (Tektronix DPO71254) using a sample rate of 25 MSample/s, are off-line processed into a single data stream for the acquisition of 4-D image. Fig. 2(a) shows the photo of top-view of our APD with a 40  $\mu$ m window diameter. Fig. 2 (b) to (d) represents the measured bias dependent photocurrent and dark currents, optical-to-electrical (O-E) frequency responses, and dc

saturation current of these APDs, respectively. We can clearly see that under a moderate optical LO pumping power (0.25 mW), which is close to the optimal value to obtain the highest S/N ratio for our demonstrated 4-D LiDAR system, the measured 3-dB optical-to-electrical (O-E) bandwidth can reach around 3 GHz with a high responsivity (2.9 A/W at 0.9 V<sub>br</sub>). Such a bandwidth is wide enough to cover the chosen IF at 2.4 GHz. Besides, the output saturation current is as high as over 5 mA, which can satisfy the pumping of optimal optical LO power at mW level. For more details about the device performance, the reader can refer to our previous work [4].

### III. Measurement Result:

Prior to the experiment for capturing the velocity and distance of the object to build its 4-D image, the operating conditions of the APD, i.e., bias voltage and optical LO pumping power, were optimized to obtain the highest S/N ratio for each pixel. Figure 3 (a) to (c) shows the bias dependent baseband spectra obtained from our APD under a fixed optical LO power at -7 dBm. As can be seen, the highest S/N ratio happens at around 0.9 V<sub>br</sub>. When the bias is further increased to 0.95 V<sub>br</sub>, the noise floor increases significantly. Figure 3 (d) to (f) shows the optical power dependent baseband spectra measured using a commercially available p-i-n PDs based Rx. Obviously, p-i-n PD shows a less S/N ratio (7.8 vs. 9 dB) than that of home-made APDs under the same optimal LO pumping power at -7 dBm. Such optimized power value is determined by the saturation of our RF SILO loop, which has a high sensitivity for weak signal detection and this in turn limits the magnitude of input signal from APD or PD. The capability of the systems for simultaneously sensing the distance and the velocity is tested using objects including the symbols I, ♡, and U which are made of Styrofoam and wrapped with retroreflective tape, as shown in Fig. 4. The ♡ shape object is placed on a motorized linear stage which moves at a given speed, while the I and U remains static. Even though the ♡ shape object is moving, the relative distances to the I, ♡, and U are set to 2, 7, and 12 cm, respectively, during the measurement. Note that the azimuth and elevation in the 4D measurement are obtained by scanning 40 by 40 pixels in this work. Figs. 5 (a) and (b) show plots of the measured images of distance and motion when the velocity of the ♡ shape object is 40 mm/s. As can be seen, some pixels show no image because they have been mistakenly determined to be part of the background, probably because of non-ideal reflection. Moreover, the APD exhibits a much better quality of 4-D image. To further improve the sensitivity of sensing velocity, it is possible to measure the velocity using a continuous wave (CW) laser over a longer FFT interval and consecutively altering the laser operating modes between FMCW and CW could realize the measurement of distance and velocity for 4D-sensing applications [9]. Fig. 6 (a) and (b) shows a plot of the motion images of the ♡ shape using APD and p-i-n PD photoreceiver when the velocity is set to 5 μm/s, respectively. Similar to the case discussed in Fig. 5, the APD based photoreceiver exhibits superior performance to that of p-i-n PD ones in the construction of motion images for slow-moving target. The insets in Fig. 6 show the captured baseband spectra of pixels in background and objects for these two cases. We can clearly see that APD receiver can provide a larger contrast ratio between the pixels of background and object than those of p-i-n PD ones. This thus leads to an improved quality of images as discussed. To the best of the authors' knowledge, the velocity sensitivity achieved here (5 μm/sec for motion images) is the highest reported for the FMCW LiDAR-based technologies, including for an on-chip silicon photonic platform with slow-light grating (75 mm/sec, 400 mm/sec [5,6]), or photonic crystal (19 mm/sec [7]) beam scanners and phase-diversity coherent detection (1500 mm/sec) [8]. Table 1 shows the benchmark of velocity sensitivity in the reported FMCW LiDARs.

### IV. Summary:

A novel 4-D FMCW LiDAR system is demonstrated in this work. By combining a RF SILO with a high-performance APD, it can provide higher quality 4-D images than that of using traditional p-i-n PD in the receiving side. Moreover, a minor Doppler frequency shift can be detected in our demonstrated system with an unprecedented high velocity-sensitivity (5 μm/sec) for the construction of slow-moving motion images. It opens up new possibilities for the next generation of 4-D LiDARs for monitoring vital-sign information.

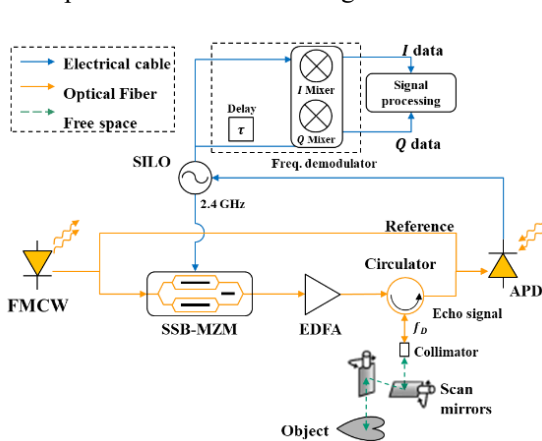


Fig. 1. The setups for the demonstrated 4-D FMCW LiDAR with RF SILO and APD receiver.

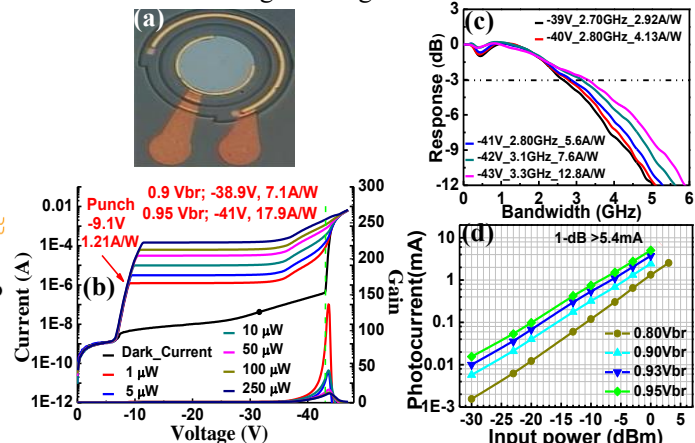


Fig. 2. (a) Top-view of the demonstrated APDs. (b) Power dependent IV and gain characteristics. (c) Bias dependent O-E frequency responses at a fixed optical power (250 μW). (d) Bias dependent DC saturation characteristics

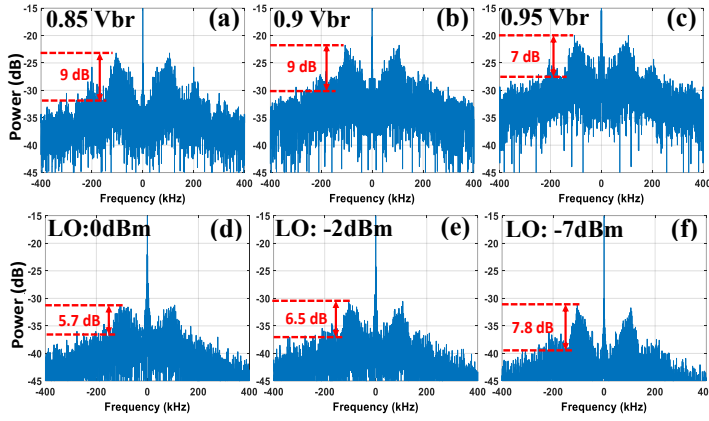


Fig. 3. (a)-(c) Bias dependent baseband spectra measured of APD at a fixed -7 dBm LO power. (d)-(f) LO power dependent baseband spectra for p-i-n PD.

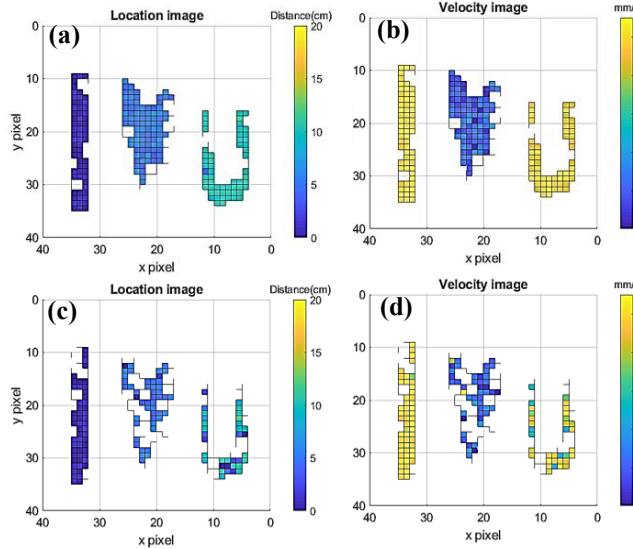


Fig. 5. The captured 4-D image using (a) (b) APD and (c) (d) p-i-n PD at 40 mm/sec.

TABLE 1  
VELOCITY SENSITIVITY OF DIFFERENT 4D FMCW LiDARS

S.No.	Measured Velocity (mm/sec)	Technology used	References
1	75	On-chip Si-Photonics Platform	5
2	400	Si Photonics Slow Light Grating	6
3	19	Si-photonics crystal beam scanner	7
4	1500	Phase-diversity coherent detection	8
5	0.005	Our cascaded M-layer APD with SILO	This work

## V. Reference:

- [1] W. -C. Su, *et al.*, "Stepped-Frequency Continuous-Wave Radar With Self-Injection-Locking Technology for Monitoring Multiple Human Vital Signs," *IEEE Trans. on Microwave Theory and Techniques*, vol. 67, no. 12, pp. 5396-5405, Dec. 2019.
- [2] S. Crouch, "Velocity Measurement in Automotive Sensing: How FMCW Radar and Lidar Can Work Together," *IEEE Potentials*, vol. 39, no. 1, pp. 15-18, Feb. 2020.
- [3] F. -K. Wang, *et al.*, "Review of Self-Injection-Locked Radar Systems for Noncontact Detection of Vital Signs," *IEEE J. of Electromagnetics, RF and Microwaves in Medicine and Biology*, vol. 4, no. 4, pp. 294-307, Dec. 2020.
- [4] Z. Ahmad, *et al.*, "High-Power and High-Responsivity Avalanche Photodiodes for Self-Heterodyne FMCW Lidar System Applications," *IEEE Access*, vol. 9, pp. 85661-85671, Jun. 2021.
- [5] C.V. Poultan, *et al.*, "Coherent solid-state LIDAR with silicon photonic optical phased arrays," *Opt. Lett.*, vol. 42, no. 20, pp. 4091-4094, Oct. 2017.
- [6] T. Baba, *et al.*, "Silicon Photonics FMCW LiDAR Chip with a Slow-Light Grating Beam Scanner," *IEEE J. of Sel. Topics in Quantum Electron.*, vol. 28, no. 5, pp. 1-8, Oct. 2022.
- [7] S. Suyama, *et al.*, "Doppler velocimeter and vibrometer FMCW LiDAR with Si photonic crystal beam scanner," *Opt. Express*, vol. 29, no. 19, pp.30727-30734, Sep. 2021.
- [8] Z. Xu, *et al.*, "FMCW Lidar Using Phase-Diversity Coherent Detection to Avoid Signal Aliasing," *IEEE Photon. Technology Letter.*, vol. 31, no. 22, pp. 1822-1825, Nov. 2019.
- [9] S. Gao, *et al.*, "Complex-optical-field lidar system for range and vector velocity measurement," *Opt. Express*, vol. 20, no. 23, pp. 25867-25875, Nov. 2012.

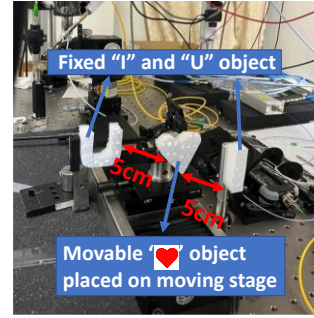


Fig. 4. Object under test.

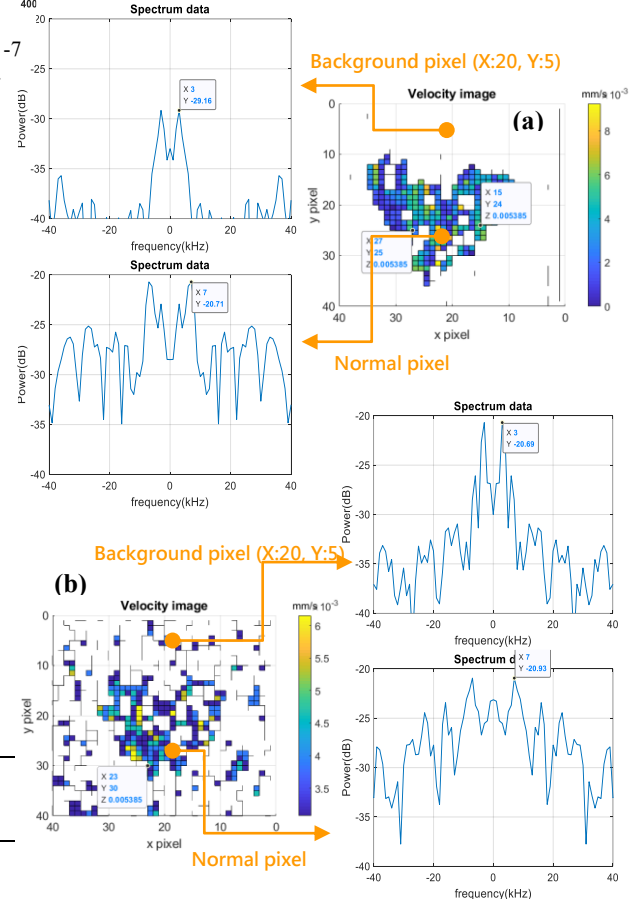


Fig. 6. The captured motion image using (a) APD and (b) p-i-n PD at the 5  $\mu$ m/sec moving speed of target. The insets show the measured baseband spectra in their pixels.